

A LAND SURFACE EMISSIVITY DATABASE FOR CONICALLY SCANNING MICROWAVE SENSORS

P1.27

Jean-Luc Moncet*, John F. Galantowicz, Pan Liang, and Alan Lipton
Atmospheric and Environmental Research Inc. (AER), Lexington, Massachusetts

1. INTRODUCTION

Accurate knowledge of local surface emissivity is required for lower tropospheric microwave remote sensing over land. Ideally, for a stand-alone microwave system, accuracies of 0.01 or less are needed to minimize the impact of cloud liquid water on temperature and water vapor retrievals and for improving surface temperature retrievals. Because surface properties may change rapidly, the emissivity database must be frequently updated. Surface emissivity may be well characterized in clear areas using collocated microwave and infrared observations although, in certain areas, terrain and surface type inhomogeneities may be a limiting factor. In cloudy (non-precipitating) conditions one must rely on temporal persistence. The use of such an approach is necessarily limited to areas for which frequency of occurrence of relatively clear measurements is higher than the rate at which surface properties change.

In this work land surface emissivity in the AMSR-E channels is retrieved from combined observations from the AMSR-E, AIRS, and MODIS instruments on the EOS/Aqua platform in relatively clear conditions. We examine the temporal variability of retrieved local surface emissivity over selected regions of the globe and provide a preliminary assessment of the usefulness of the product for cloudy microwave retrievals. Since the emissivity retrieval is sensitive to the specification of land surface temperature (LST) we have also investigated the use of different sources for LST (such as those from physical land surface models and analyses), and attempt to characterize these differences both in terms of the respective LSTs, as well as the retrieved emissivities.

2. DATABASE GENERATION

Figure 1 gives an overview of the end-to-end processing flow for emissivity derivation. Primary inputs are the AMSR radiances footprint matched to resolution 2 (51x29 km except 6 GHz 75x43 km) and their geolocation data, MODIS Level 3 1 km LST, and NCEP/GDAS atmospheric profiles. MODIS LSTs are averaged over the area of each AMSR field-of-view (FOV) and NCEP atmospheric profiles are time-interpolated to each FOV observation time and vertically interpolated to the

radiative transfer model's pressure levels. In clear-sky conditions (according to MODIS LST quality flags), the retrieval background (covariance and first-guess) is built from the ancillary inputs and the core 1-D VAR retrieval model (Moncet et al., 2001) is run in a direct emissivity inversion mode (i.e., LST and atmosphere first guess absolutely constrain emissivity retrieval). In cloudy-sky conditions (i.e., MODIS LST is unavailable), first guess emissivities and error characteristics are drawn from the database and LST is added as an additional retrievable. In either mode, retrieval products are interpolated to a fixed earth grid.

Optionally, LST inputs may come from ISCCP, AGRMET, or other models and atmospheric profile inputs may come from AIRS retrievals. Comparisons between LST sources are described below. MODIS cloud mask data is currently incorporated through the MODIS LST QC inputs.

In addition to AMSR-channel emissivities, the gridded database includes LST, CLW retrievals for cloudy-condition retrievals, and quality flags including inhomogeneous surfaces (leading to high variability in gridded products), transient event detection (precipitation etc.), persistence of day-night variability (suggesting LST cross-talk or view azimuth dependence), unscreened cloud detection, large precipitable water errors, missing data, and retrieval mode (e.g., clear-sky with external LST or cloudy sky with emissivity database lookup).

To-date we have processed two months of global data—July and October 2003—for cloud-free conditions only. After resolution of identified technical and scientific issues, an entire calendar year's worth of data will be analyzed with cloud-free retrievals used to augment cloudy retrievals wherever emissivities are stable in time. The remainder of the paper describes methods for indirect product verification and pending questions.

3. PRODUCT VERIFICATION

Figure 2 shows an example of a global emissivity database product—the AMSR 19 GHz V-pol. month-average emissivity for July 2003. Since direct verification of emissivity products with *in situ* data is not possible, a number of indirect verification methods have been developed. Indirect product verification plans include consistency checks with AMSR soil moisture product anomalies, consistency with SSMI-derived emissivities, day-to-day temporal stability (outside of precipitation events etc.), capture of the diurnal LST cycle, improvement in CLW detection over land (via comparison with cloud maps from AVHRR etc.),

* Corresponding author address: Jean-Luc Moncet, AER, Inc, 131 Hartwell Ave, Lexington, MA 02421
Tel: 781-761-2267; e-mail: jmoncet@aer.com

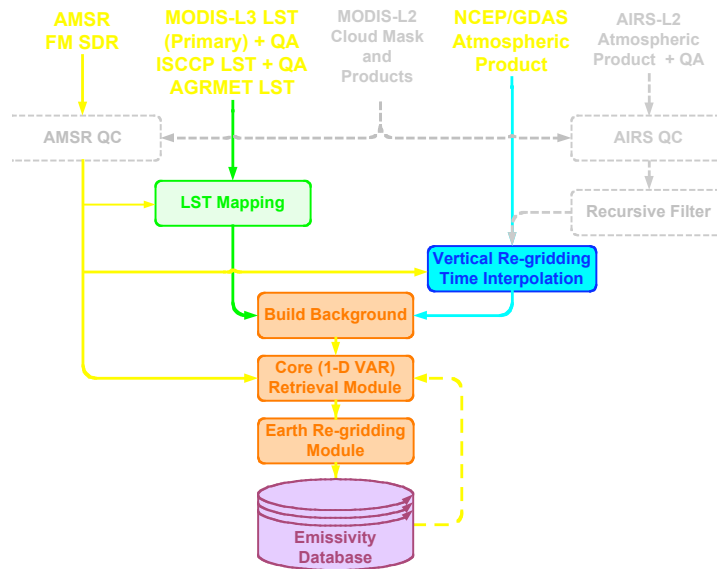


Figure 1: Overview of end-to-end data processing system. Dashed lines represent optional processes.

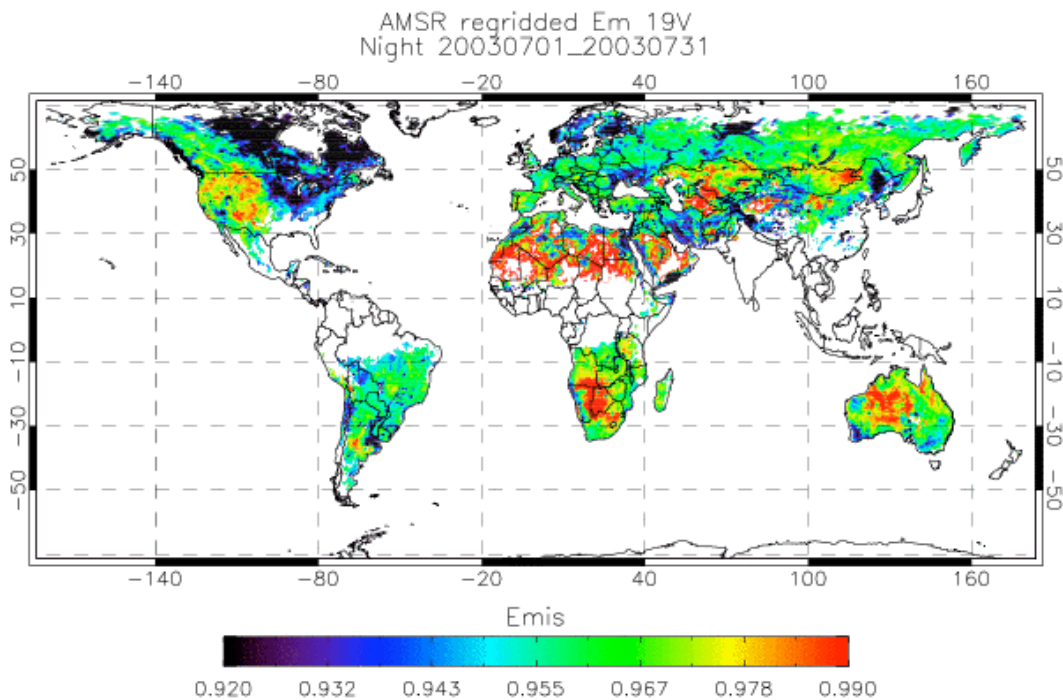


Figure 2: Month-averaged 19V emissivity from global emissivity database for July 2003, nighttime retrievals only. White areas were found to have persistent cloudiness according to MODIS cloud masks.

and radiometric and physical consistency with IR measurements.

Figure 3 shows comparison of the AMSRR July 2003 month-averaged 19H emissivity for CONUS to the same product derived by Prigent from SSM/I for 1992 (Prigent, 1997). There is good spatial correspondence between the two datasets despite

the inclusion of transient events (e.g., precipitation) in both and the difference in years and overpass times (AMSRR 0200 vs. SSM/I 0530-0930). We are considering adding SSM/I data to the processing stream to provide independent emissivity estimates at ~0600 local time when thermal gradients near the surface and across the scene are reduced.

Figure 4 gives an example of emissivity change detection through inter-comparison of emissivity and AMSR soil moisture product anomaly time series. Because clouds were not screened in this test run, high-emissivity anomalies can be attributed to low-biased MODIS LST inputs caused by the presence of clouds. On July 8 (third panel,

circled) a low-emissivity anomaly in Oregon matches a high anomaly in the AMSR soil moisture product. Furthermore, a cloud detected to the northeast of the anomaly is thought to be the remnant of the precipitating cloud responsible for the elevated soil moisture. Detection of the event and the lack of other such anomalies over this time

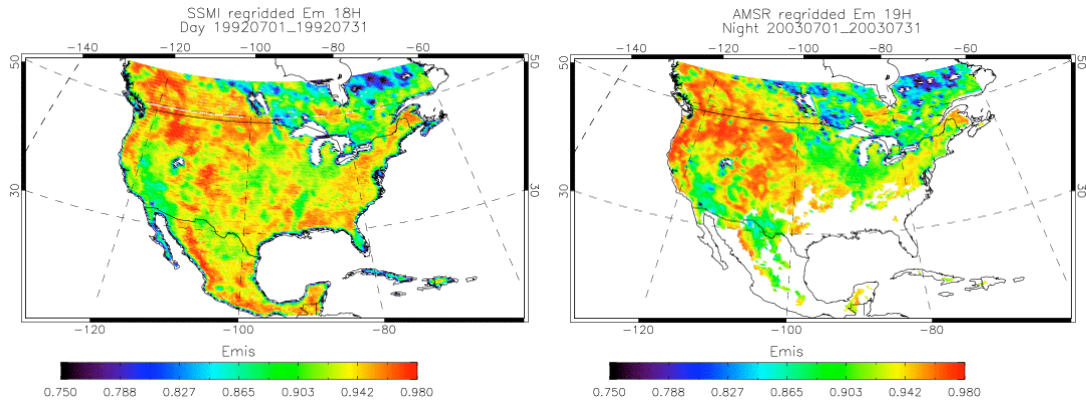


Figure 3: July month-average 19H emissivity from July 1992 (left; Prigent, 1998) and retrieval over July 2003 from AMSR data.

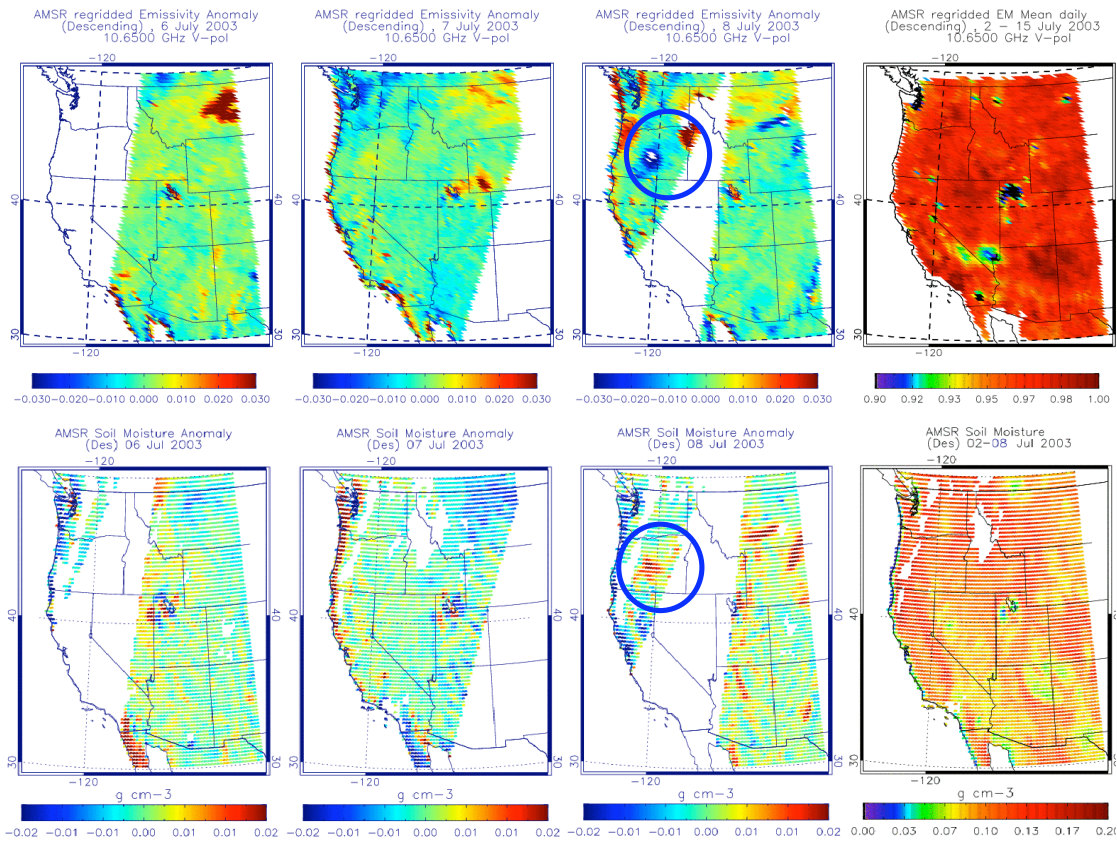


Figure 4: Top: Retrieved AMSR 10V emissivity anomaly for 7/6-7/8 2003 and 7/2-7/15 emissivity mean. Bottom: AMSR soil moisture product anomalies and 2-week soil moisture mean for the same time period. Note that clouds were *not* screened in the emissivity product accounting for some large positive emissivity anomalies.

period suggest that the emissivity database will have good skill in flagging temporal emissivity anomalies and providing a record of emissivity stability useful for retrievals at subsequent times when the database is to be used for the emissivity first-guess.

4. PENDING QUESTIONS

A number of questions have been identified from analysis of the two months of data already processed leading to changes in the processing system and development of quality assessment methods for the emissivity database products.

Local LST biases: Disagreement between various LST sources (MODIS, GDAS/NOAH LSM, GRMET, AIRS, ISCCP) is especially bad during the daytime. Our current focus is on identification of regions where differences are minimal in order to better understand sources of disagreement. Day-night emissivity retrieval stability (excluding transient events) can be used as a metric for LST quality. Figure 5 shows comparisons between the various model products and MODIS LST.

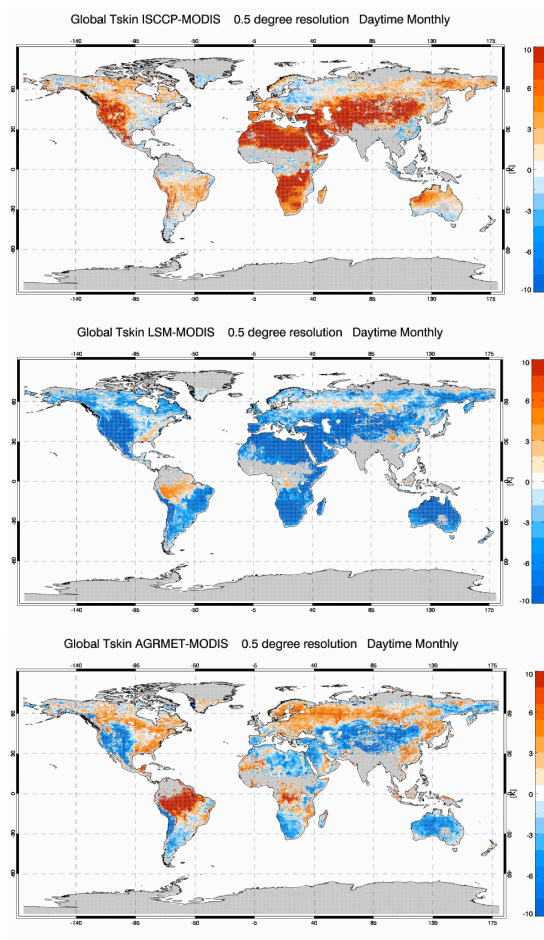


Figure 5: July 2003 monthly-averaged differences between the ISCCP, NOAA-LSM, and AGRMET 1400 hr skin temperatures and MODIS LST.

Penetration depth and subsurface temperature gradients: Skin-to-subsurface temperature gradients are expected to be high at AMSR observation times (~0200 and 1400 local equator crossing times). We are currently working on approaches that would account for the frequency-dependence in microwave emitting temperatures where subsurface penetration is high. For example, some model LST products may better represent the effective emitting temperature of microwave radiances because they are parameterizations of bulk near-surface conditions. Further analyses are discussed below.

Earth-gridding and spatial variability errors: Small changes in geolocation can cause emissivity variability, primarily around water bodies or other large, contrasting features. Figure 6 shows that most of the areas of high variability in the western US over a 1-week period were due to identifiable water bodies. We have developed a more accurate procedure for mapping AMSR data to our earth grid and we also plan to flag heterogeneous areas.

Emissivity retrieval in regions of quasi-permanent cloud cover: We are examining the reliability of ISCCP temperatures in these regions as well as further evaluating the reliability of the MODIS cloud mask.

Dew: We do not expect dew to be widespread at the AMSR observation times. We may include a flag for possible dew based on meteorological conditions.

AMSR calibration: Our examination of possible

Standard deviation of AMSR regridded emissivity (Descending) 2 - 8 July 2003

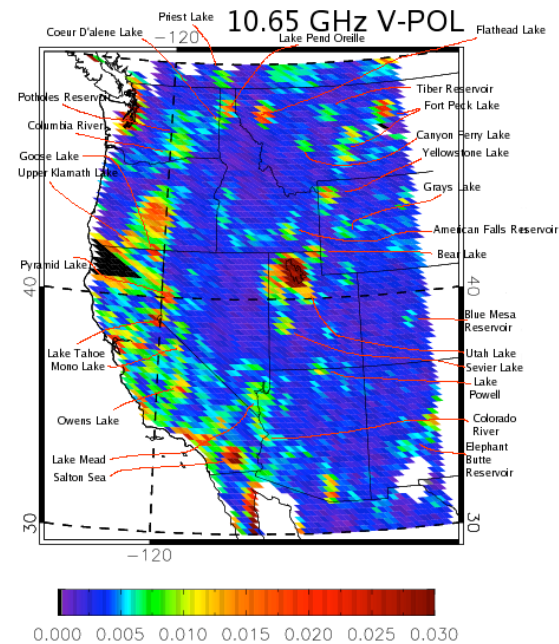


Figure 6: Variability in retrieved 10V emissivity showing the correspondence between water bodies and high variability.

effects of calibration errors on retrievals suggests that other issues (above) are more likely the cause of anomalous observations.

MODIS cloud mask: Clouds appear to be over-estimated especially in tropical nighttime scenes.

5. MICROWAVE PENETRATION DEPTH ANALYSIS

Figure 7 shows a map of the night-day difference in 19V/11V AMSR brightness temperature ratio. Where the difference is small there is little change in the spectral slope of the brightness temperatures over the course of the day. Where there are large negative (blue) differences, the 19 GHz brightness temperature exhibits a larger day-night change than 10 GHz. Since these large changes occur in drier areas, we expect that they are primarily due to differences between the effective depth of emission at 10 and 19 GHz and the presence of significant temperature gradients over those depths.

As a test of this hypothesis, we simulated temperature profiles in rocks and dry sand soil surfaces using a heat and moisture transfer model with land-atmosphere interaction. Two rocks types were characterized by high (5.7 W/mK) and low (2.93) thermal conductivity and low albedo (0.16) and the sand soil by lower thermal conductivity (due to air within the soil) but high albedo (0.45). The circle in Figure 7 indicates a region where sand dunes are surrounded by more rocky surface cover. (The dunes cover an extensive “n” shaped area.)

From this region, we identified sand and rock-dominated grid cells and estimated the day-night difference in effective emitting temperature from AMSR brightness temperatures and nighttime emissivity database retrievals. After scaling the simulations to match the observed MODIS day-night skin temperature temperature change (22 K in both the sand and rock) we used the simulations to estimate the emitting depth needed to produce the observed temperature cycles. These depths are plotted for each surface type along with the full profile day-night temperature changes in Figure 8. For example, the 10 GHz day-night AMSR temperature change for sand was near zero corresponding to a depth of at least 20 cm in the simulations (the average of the first three points closest to zero is plotted). In contrast, the estimated 10 GHz penetration depth in rock is ~8 cm. A similar analysis by Prigent (1999) found depths up to 15 cm at 19 GHz, which is comparable to our 18 cm depth estimated for sand. Further use of thermal simulations will be useful for both quantifying the magnitude of penetration depth effects relative to other sources of bias and for developing measures for

6. CONCLUSIONS

We have described preliminary results from a system for deriving microwave emissivities from AMSR-E and ancillary measurements. In addition to July and October 2003, we plan to add two more months to our provisional processing stream

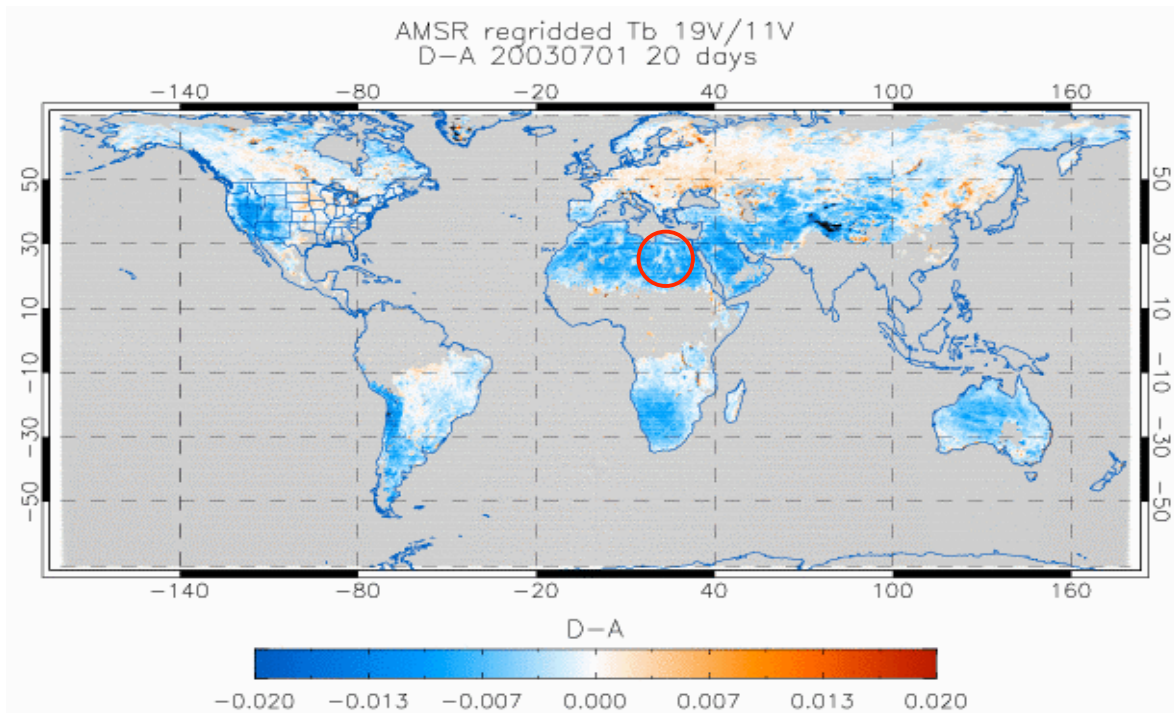


Figure 7: Night-day difference in 19V/11V AMSR brightness temperature ratio averaged over 20 days in July 2003.

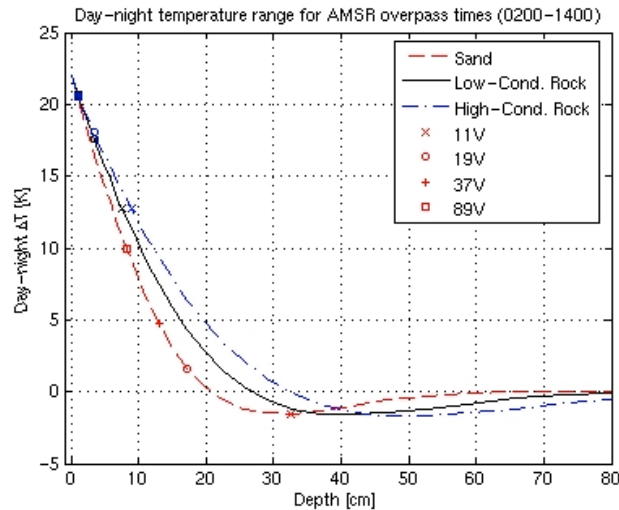


Figure 8: Day-night temperature change as a function of depth for simulated sand and rock types scaled by MODIS skin temperature observations. Symbols mark depths where the temperature changes match estimated effective emitting temperature changes at AMSR 11, 19, 37, and 85 GHz derived from areas in Figure 7 where sand and rock types were predominant.

(January and April 2003) and continue to build a database of test cases from particular grid cells covering problem areas (e.g., cloud contamination, penetration depth, re-gridding errors, LST errors, AMSR noise, atmospheric profile errors) as well as areas where retrieval confidence is high. Our goal is to begin processing of a full year of data beginning in early 2006.

The near-term objective is to build a prototype system for estimating the quality of clear-sky surface emissivities that might be used for cloudy-sky AMSR retrievals. We plan to develop radiative transfer models to confirm our estimates of emission depths based on thermal modeling. Areas where persistent nighttime cloud flags are suspected to be erroneous will be addressed by conducting clear-sky nighttime retrievals then using the retrieved emissivities to perform a cloud-sky retrieval at a time when cloudiness is confirmed (e.g., daytime). If the retrieved cloud liquid water is near-zero despite the presence of clouds then it is likely that there was cloud contamination in the nighttime scenes when the emissivities were derived.

7. REFERENCES

- Moncet, J-L., Boukabara, S., Lipton, A., Galantowicz, J., Rieu-Isaacs, H., Hegarty, J., Liu, X., Lynch, R., Snell, H., Algorithm Theoretical Basis Document (ATBD) for the Conical-Scanning Microwave Imager/Sounder (CMIS) Environmental Data Records (EDRs) Volume 2: Core Physical Inversion Module, Version 1.4, March 15, 2001, http://140.90.86.6/IPOarchive/SCI/atbd/ATBD_V.02_CorePhysicalInversionModule.pdf
- Prigent, C., Rossow, W. B., Matthews, E., and Marticorena, B., Microwave radiometric signatures of different surface types in deserts, *J. Geophys. Res.*, **104**, D10, pp. 12147-12158, 1999.
- Prigent, C., Rossow, W. B., and Matthews, E., Global maps of microwave land surface emissivities: Potential for land surface characterization, *Radio Sci.*, **33**, pp. 745-751, 1998.